

Superconducting transitions from the pseudogap state: d -wave symmetry, lattice, and low-dimensional effects

Qijin Chen, Ioan Kosztin, Boldizsár Jankó, and K. Levin

The James Franck Institute, University of Chicago, 5640 South Ellis Avenue, Chicago, Illinois 60637

(Received 4 May 1998)

We investigate the behavior of the superconducting transition temperature within a previously developed BCS Bose-Einstein crossover picture. This picture, based on a decoupling scheme of Kadanoff and Martin, further extended by Patton, can be used to derive a simple form for the superconducting transition temperature in the presence of a pseudogap. We extend previous work which addressed the case of s -wave pairing in jellium, to explore the solutions for T_c as a function of variable coupling in more physically relevant situations. We thereby ascertain the effects of reduced dimensionality, periodic lattices, and a d -wave pairing interaction. Implications for the cuprate superconductors are discussed. [S0163-1829(99)01110-8]

I. INTRODUCTION

The concept of a smooth evolution from a BCS description of superconductivity to that of Bose-Einstein condensation (BEC) dates back to Eagles¹ and to Leggett.² The latter addressed this problem at zero temperature in the context of p -wave pairing in He³. Nozières and Schmitt-Rink³ (NSR) extended Leggett's formalism to calculations of T_c and, for the case of a jellium gas, found a continuous variation from the BCS exponential dependence (on coupling constant g) to the Bose-Einstein asymptote, at large g . Uemura⁴ and, independently, Randeria⁵ and Micnas⁶ and their respective co-workers applied this BCS Bose-Einstein crossover picture to the high-temperature superconductors, which, because of their short coherence length, were claimed to correspond to intermediate values of the coupling. It was, subsequently, argued by these and other groups that the pseudogap (normal) state of the cuprates was naturally associated with this intermediate coupling regime. Since then, a large number of papers⁷⁻⁹ have been written on the crossover problem and the related pseudogap state.

The application of these crossover theories to the cuprates is made complex by a number of important factors which involve quasi-two dimensionality, lattice periodicity, and, finally, the introduction of d -wave symmetry in the pairing interaction. It is the goal of the present paper to discuss these three effects in the context of a many-body-theoretic approach to the crossover problem, based on earlier work by Kadanoff and Martin,¹⁰ and extended by Patton.¹¹ A major advantage of this scheme is that it reduces to BCS theory in the limit of weak coupling. Our principal contributions^{12,13} to the larger body of work on the BCS-Bose Einstein crossover have been based on s -wave pairing in three-dimensional jellium. In the context of this diagrammatic approach we have established that (i) there is a breakdown (for $T < T^*$) of the Fermi liquid at intermediate g , which roughly coincides with the onset of long lived (i.e., resonant) pairs and (ii) that this breakdown has characteristic pseudogap features, such as a depressed density of states at Fermi energy E_F , as well as a two-peaked spectral function. The pseudogap amplitude Δ_{pg} can, moreover, be quantified. (iii) We have examined the superconducting instability associated with this pseudogap state and determined the three self-consistent, coupled equa-

tions which must be satisfied for the interrelated quantities T_c , μ , and $\Delta_{pg}(T_c)$. (iv) In the process we have presented a quantitative phase diagram for T_c and T^* as a function of the coupling g .

Various aspects of low dimensionality, lattice effects, and non- s -wave pairing interactions have been addressed in the literature within a crossover scenario. Schmitt-Rink, Varma, and Ruckenstein¹⁴ applied the NSR approach to two-dimensional systems and found a breakdown of the Fermi liquid even for arbitrarily weak coupling g . This was manifested as a negative chemical potential μ , which occurred in conjunction with $T_c = 0$. Serene¹⁵ suggested that this breakdown was an artifact of the NSR scheme, which is not conserving.¹⁶ Yamada and co-workers¹⁷ introduced a diagrammatic "mode-mode coupling" scheme, following similar work on related magnetic problems, and they found that μ was properly positive at weak coupling, while T_c remained zero, as expected. However, they were unable to find a continuous crossover between the limits of very strong and weak interactions.

Lattice effects were discussed in the original Nozières and Schmitt-Rink paper (and later by Belkhir and Randeria¹⁸). These authors noted that the T_c calculations of the jellium case, could not be readily extended to the lattice, at least in the strong coupling regime. This difficulty came from a variety of issues, among which, it was claimed, was the neglect of interactions between pairs of composite fermions. In addition there is a reduction in the effective pair hopping matrix element or kinetic energy. These combined effects conspire so that T_c is expected to vanish at arbitrarily large g , in contrast to the transition in the Bose-Einstein ideal gas. Demonstrations of this effect, in the negative U Hubbard model, came later, through Monte Carlo studies,¹⁹ as well as from additional analytic work based on the coherent potential approximation.²⁰

The role of non- s -wave pairing symmetry was initially investigated by Leggett and, subsequently, by other groups²¹ which addressed jellium models. It was noted² that in the strong coupling limit the effects of an anisotropic order parameter are absent in the excitation spectrum, so that there can be no gap nodes in the bosonic regime. d -wave pairing on a lattice is not yet amenable to Monte Carlo approaches because of the fermion sign problem. There have been, nev-

ertheless, some numerical solutions which address electronic spectral functions, based on the “fluctuation exchange approximation” (FLEX) for the lattice d -wave case.²² Because these were applied to a strictly two-dimensional (2D) model there was no discussion of the behavior of T_c in the more general context of the crossover problem.

The results of the present paper, in which T_c is computed as a function of g , can be put into the context of this background literature. Here we arrive at a crossover scheme which in the strict 2D limit yields $T_c=0$ and in which μ smoothly interpolates from E_F to large negative values in the jellium case, as the coupling varies from weak to strong. Lattice effects yield a vanishing strong coupling limit for T_c , associated with a reduction in the effective kinetic energy of the bosons or pairs. The d -wave case on a lattice is found to be different from the s -wave lattice case in one significant respect: we find that superconductivity disappears at relatively smaller values of g , as a result of d -wave symmetry; the pair size cannot be less than a lattice spacing so that the pairs interact more strongly. As a consequence their mobility is suppressed. Consequently, the bosonic regime is essentially never reached for the d -wave case.²³ The implications of this observation and other aspects of these calculations for the underdoped cuprates are briefly addressed at the end of this paper.

II. THEORETICAL FRAMEWORK

We consider a generic system of fermions characterized by an effective, short range pairing interaction with Hamiltonian

$$\mathcal{H} = \sum_{\mathbf{k}\sigma} \epsilon_{\mathbf{k}} c_{\mathbf{k}\sigma}^\dagger c_{\mathbf{k}\sigma} + \sum_{\mathbf{k}\mathbf{k}'\mathbf{q}} V_{\mathbf{k},\mathbf{k}'} c_{\mathbf{k}+\mathbf{q}/2\uparrow}^\dagger c_{-\mathbf{k}+\mathbf{q}/2\downarrow}^\dagger c_{-\mathbf{k}'+\mathbf{q}/2\downarrow} c_{\mathbf{k}'+\mathbf{q}/2\uparrow}, \quad (1)$$

where $c_{\mathbf{k}\sigma}^\dagger$ creates a particle in the momentum state \mathbf{k} with spin σ , and $\epsilon_{\mathbf{k}}$ is the energy dispersion measured from the chemical potential μ (we take $\hbar = k_B = 1$). For simplicity, we assume a separable pairing interaction $V_{\mathbf{k},\mathbf{k}'} = g \varphi_{\mathbf{k}} \varphi_{\mathbf{k}'}$, where $g = -|g|$ is the coupling strength; the momentum dependence of the function $\varphi_{\mathbf{k}}$, which reflects the pairing anisotropy, will be specified below.

In order to establish notation and to make clear our approximations, in what follows we provide a brief description of our formalism. This approach is based on the correlation function (or Green’s function equation of motion) formulation of the “pairing approximation” originally discussed by Kadanoff and Martin¹⁰ and later extended by Patton.¹¹ The system can be characterized by the one- and two-particle Green’s functions which, in real space, obey the following equations:¹⁰

$$G(1-1') = G_0(1-1') + \int d\bar{1}d\bar{2}G_0(1-\bar{1})V(\bar{1}-\bar{2})G_2(\bar{1}\bar{2};1'2^+), \quad (2a)$$

$$C_2(12;1'2') = - \int d\bar{1}d\bar{2}G(1-\bar{1})G_0(2-\bar{2}) \times V(\bar{1}-\bar{2})G_2(\bar{1}\bar{2};1'2'), \quad (2b)$$

where the two-particle correlation function C_2 is given by

$$C_2(12;1'2') = G_2(12;1'2') - G(1-1')G_0(2-2') \quad (2c)$$

and, for brevity, we have used a four vector notation $1 \equiv (\mathbf{r}, \tau)$, etc. While Eq. (2a) is exact, Eqs. (2b) and (2c) are approximate; these equations were originally proposed by Kadanoff and Martin^{10,24} [see their Eqs. (2.6) and, most importantly, Eq. (2.29)] as a simple decoupling scheme for the three-particle Green’s function.

This approach is primarily motivated by the observation that it yields the results of BCS theory, in the weak coupling limit. It is convenient to express the correlation function C_2 in terms of a T matrix (or *pair propagator*) via the definition

$$C_2(12;1'2') = \int d\bar{1}d\bar{2}d\bar{1}'d\bar{2}'G(1-\bar{1})G_0(2-\bar{2}) \times t(\bar{1}\bar{2};\bar{1}'\bar{2}')G(\bar{1}'-1')G_0(\bar{2}'-2'). \quad (3)$$

Taking the Fourier transform of Eqs. (2) and (3), and noticing that for our separable interaction the T matrix can be written as $t(K,K';Q) = t(Q)\varphi_{\mathbf{k}}\varphi_{\mathbf{k}'}$, after some straightforward algebra we obtain the following equations¹¹ for the self-energy:

$$\Sigma(K) = G_0^{-1}(K) - G^{-1}(K) = \sum_Q t(Q)G_0(Q-K)\varphi_{\mathbf{k}-\mathbf{q}/2}^2, \quad (4a)$$

and the T matrix

$$g = [1 + g\chi(Q)]t(Q), \quad (4b)$$

where

$$\chi(Q) = \sum_K G(K)G_0(Q-K)\varphi_{\mathbf{k}-\mathbf{q}/2}^2 \quad (4c)$$

is the pair susceptibility. Here, $G_0(K) = 1/(i\omega - \epsilon_{\mathbf{k}})$ is the bare propagator, and $K \equiv (\mathbf{k}, i\omega)$, $\Sigma_K \equiv T\Sigma_{\mathbf{k},i\omega}$, etc., with Ω/ω denoting the even/odd Matsubara frequencies. Together with the particle number equation

$$n = 2 \sum_K G(K), \quad (4d)$$

Eqs. (4) form a complete set which, for a given g and T , need to be solved self-consistently for $\Sigma(K)$, $t(Q)$, and the chemical potential μ . Equations (4) represent the basis of the present theory and can be regarded as a generalized BCS

theory in which pair correlations are explicitly taken into account in the normal state ($T > T_c$) in a self-consistent fashion.

This approach has implications for the superconducting state as well. The presence of (noncritical) pair fluctuations in the superconducting state ($T < T_c$) leads to progressively stronger deviations from BCS theory as the coupling is increased. However, this standard (BCS) theory is embedded in Eqs. (4) when the T matrix is given by

$$t_{sc}(Q) = \begin{cases} 0 & \text{for } T > T_c, \\ -(|\Delta_{sc}|^2/T)\delta(Q) & \text{for } T < T_c, \end{cases} \quad (5)$$

where Δ_{sc} is the superconducting order parameter. Inserting Eq. (5) into Eqs. (4) one obtains (i) the usual BCS self-energy $\Sigma_{BCS}(K) = |\Delta_{sc}|^2 \varphi_{\mathbf{k}}^2 / (i\omega + \epsilon_{-\mathbf{k}})$ and (ii) gap equation $0 = 1 + g\chi(0) = 1 + g \sum_K |\Delta_{sc}|^2 \varphi_{\mathbf{k}}^2 / (\omega^2 + E_{\mathbf{k}}^2)$, where $E_{\mathbf{k}} = \sqrt{\epsilon_{\mathbf{k}}^2 + |\Delta_{sc}|^2 \varphi_{\mathbf{k}}^2}$ is the energy dispersion of the quasiparticles. The delta function in $t_{sc}(Q)$ leads to the usual (Gor'kov) factorization of the correlation function $C_2(K, K') = F(K)F(K')$, where the anomalous Green's function $F(K) = \Delta_{sc} \varphi_{\mathbf{k}} G_0(-K)G(K)$.

Under more general circumstances, when pair fluctuations cannot be neglected, the self-consistent T matrix in Eqs. (4) can be written as

$$t(Q) = t_{sc}(Q) + t_{pg}(Q), \quad (6a)$$

$$t_{pg}(Q) = \frac{g}{1 + g\chi(Q)}, \quad (6b)$$

where $t_{pg}(Q)$ is the ‘‘regular’’ (or pseudogap) contribution [cf. Eq. (4b)], which should be associated with (noncritical) pair fluctuations which persist both above and below T_c . At the high temperatures of the normal state, $t_{pg}(Q)$ is finite at all Q . As the temperature is lowered $t_{pg}(Q)$ develops a resonant structure corresponding to metastable or long lived pairs. Precisely at T_c , this quantity becomes divergent for $Q=0$, in accord with the Thouless criterion for a superconducting pairing instability. Once the temperature is less than T_c , a nonzero superconducting order parameter Δ_{sc} is established which obeys the (gap) equation $1 + g\chi(0; T) = 0$. It is important to stress that the same critical temperature is obtained either when approached from the normal state (using the Thouless criterion)

$$t_{pg}^{-1}(0) = g^{-1} + \chi(0; T_c) = 0 \quad (7)$$

or when approached within the superconducting state by setting $\Delta_{sc} = 0$ within the gap equation.

The calculation of T_c can be substantially simplified by noting that at this temperature the self-energy is well approximated by¹³

$$\Sigma(K) \approx G_0(-K) \varphi_{\mathbf{k}}^2 \sum_Q t_{pg}(Q). \quad (8a)$$

This approximation is *highly nontrivial* and establishing its validity requires detailed numerical calculations which are presented elsewhere.¹³ It should be stressed that Eq. (8a) cannot be written down on analytical grounds alone. It is a consequence of a numerical iterative solution¹³ of Eqs. (4)

and obtains when the T matrix contains a divergence. In the pseudogap phase Eq. (8a) is no longer a valid approximation to Eq. (4a). Indeed, one may arrive at some apparent inconsistencies if this approximation is used above T_c . It follows from Eq. (8a) that at T_c , the self-energy has the same symmetry as in the superconducting state. However, it can be seen from the exact Eq. (4a), that the pairing symmetry factor $\varphi_{\mathbf{k}}$ cannot, in general, be extracted from inside the integral. When the integration is properly performed, the anisotropy at higher temperature will generally be different from that at T_c . This important consequence, which may be relevant to experiment,²⁵ would not follow if Eq. (8a) were incorrectly extended beyond its regime of validity.

The self-energy can be rewritten as

$$\Sigma(K) \approx \frac{\Delta_{pg}^2 \varphi_{\mathbf{k}}^2}{i\omega + \epsilon_{-\mathbf{k}}}, \quad (8b)$$

where the pseudogap parameter is defined as

$$\Delta_{pg}^2 \equiv - \sum_Q t_{pg}(Q) = - \sum_{\mathbf{q}} \int_{-\infty}^{\infty} \frac{d\Omega}{\pi} b(\Omega) \text{Im } t_{\mathbf{q}, \Omega} \quad (9a)$$

in terms of the Bose function $b(\Omega)$. Here, and in what follows, we use the notation Δ_{pg} to represent the amplitude of the pseudogap at T_c , while the momentum dependence is given by $\Delta_{\mathbf{k}} = \Delta_{pg} \varphi_{\mathbf{k}}$. The simple BCS-like form of the self-energy (8b) allows us to express Eqs. (7) and (4d) as

$$t_{pg}^{-1}(0) = g^{-1} + \sum_{\mathbf{k}} \frac{1 - 2f(E_{\mathbf{k}})}{2E_{\mathbf{k}}} \varphi_{\mathbf{k}}^2 = 0 \quad (9b)$$

and

$$n = 2 \sum_{\mathbf{k}} \left[v_{\mathbf{k}}^2 + \frac{\epsilon_{\mathbf{k}}}{E_{\mathbf{k}}} f(E_{\mathbf{k}}) \right], \quad (9c)$$

where $v_{\mathbf{k}}^2 = \frac{1}{2}(1 - \epsilon_{\mathbf{k}}/E_{\mathbf{k}})$, $u_{\mathbf{k}}^2 = \frac{1}{2}(1 + \epsilon_{\mathbf{k}}/E_{\mathbf{k}})$, and $f(E)$ is the Fermi function. The complete set of Eqs. (9), which were previously established in a slightly different form in Ref. 26, must be solved self-consistently in order to obtain T_c , μ , and Δ_{pg} as a function of g and n .

The imaginary component of the T matrix which appears in the pseudogap equation (9a) can be directly calculated by inserting Eq. (8b) into Eqs. (6b) and (4c). However, extensive numerical calculations^{13,27} show that as T_c is approached from above, one can simplify this procedure considerably and, at the same time, obtain considerable physical insight. For the purposes of calculating quantities such as Δ_{pg}^2 (which involve integrals over the T matrix), it suffices to approximate the T matrix near T_c by its values at small Ω and \mathbf{q} . We derive the appropriate form by noting that the inverse of the analytically continued function can be written as

$$\text{Re } t_{\mathbf{q}, \Omega}^{-1} \approx a'_0(\Omega - \Omega_{\mathbf{q}}),$$

$$\text{Im } t_{\mathbf{q}, \Omega}^{-1} \approx a''_0 \Omega,$$

where $\Omega_{\mathbf{q}}$ can be naturally interpreted as an energy dispersion of pairs of fermions. Here the parameters a'_0 and a''_0 are essentially constant in the relevant range of momentum and frequency. Moreover,¹³ independent of the values of g , suf-

ficiently close to T_c , we find that the ratio $\varepsilon \equiv a_0''/a_0' \ll 1$. Hence the imaginary part of the T matrix can be approximated as

$$\begin{aligned} \text{Im } t_{\mathbf{q},\Omega} &\approx - \lim_{\varepsilon \rightarrow 0} \frac{\text{Im } t_{\mathbf{q},\Omega}^{-1}}{[\text{Re } t_{\mathbf{q},\Omega}^{-1}]^2 + [\text{Im } t_{\mathbf{q},\Omega}^{-1}]^2} \\ &= - \frac{1}{a_0' \Omega} \lim_{\varepsilon \rightarrow 0} \frac{\varepsilon}{(1 - \Omega_{\mathbf{q}}/\Omega)^2 + \varepsilon^2} = - \frac{\pi}{a_0'} \delta(\Omega - \Omega_{\mathbf{q}}). \end{aligned}$$

Finally, it is useful to rewrite the approximated T matrix at T_c (for small momenta and frequencies) in a more compact form as

$$t_{\mathbf{q},\Omega} \approx \frac{a_0'^{-1}}{\Omega - \Omega_{\mathbf{q}} + i\varepsilon\Omega}. \quad (10)$$

This approximated T matrix takes the natural form of a pair ‘‘Green’s function’’ or propagator, with characteristic dispersion $\Omega_{\mathbf{q}}$. Using the inversion symmetry of the Hamiltonian we deduce that $\Omega_{\mathbf{q}}$ varies quadratically at T_c with the wave vector, as

$$\Omega_{\mathbf{q}} \approx \begin{cases} \frac{q^2}{2M^*} & \text{for 3D,} \\ \frac{q_{\parallel}^2}{2M_{\parallel}^*} + \frac{q_{\perp}^2}{2M_{\perp}^*} & \text{for quasi-2D,} \end{cases} \quad (11)$$

where M^* is the effective mass of the pairs. By quasi-2D we mean a highly anisotropic 3D system with $M_{\perp}^*/M_{\parallel}^* \gg 1$. The effective pair mass is determined by an expansion of the pair dispersion, given by

$$\begin{aligned} \Omega_{\mathbf{q}} &= - \frac{1}{a_0'} \left\{ \sum_{\mathbf{k}} \left[\frac{1 - f(E_{\mathbf{k}}) - f(\epsilon_{\mathbf{k}-\mathbf{q}})}{E_{\mathbf{k}} + \epsilon_{\mathbf{k}-\mathbf{q}}} u_{\mathbf{k}}^2 \right. \right. \\ &\quad \left. \left. - \frac{f(E_{\mathbf{k}}) - f(\epsilon_{\mathbf{k}-\mathbf{q}})}{E_{\mathbf{k}} - \epsilon_{\mathbf{k}-\mathbf{q}}} v_{\mathbf{k}}^2 \right] \varphi_{\mathbf{k}-\mathbf{q}/2}^2 - \frac{1 - 2f(E_{\mathbf{k}})}{2E_{\mathbf{k}}} \varphi_{\mathbf{k}}^2 \right\}, \end{aligned} \quad (12)$$

where

$$a_0' = \frac{1}{2\Delta_{\text{pg}}^2} \sum_{\mathbf{k}} \left[[1 - 2f(\epsilon_{\mathbf{k}})] - \frac{\epsilon_{\mathbf{k}}}{E_{\mathbf{k}}} [1 - 2f(E_{\mathbf{k}})] \right]. \quad (13)$$

We have verified numerically that the above leading order (in \mathbf{q}) contributions in Eq. (11) dominate in our subsequent calculations, so that higher order terms in the expansion can be dropped. The relationship between the effective mass of the pairs and T_c will be explored in detail in Sec. III A.

The above analysis will be applied to isotropic and anisotropic jellium with s -wave pairing, as well as to discrete lattices. In the latter case we consider both s - and d -wave symmetry of the pairing interaction $V_{\mathbf{k},\mathbf{k}'}$. The distinction between these various situations enters via the dispersion relation $\epsilon_{\mathbf{k}}$ and the symmetry factor $\varphi_{\mathbf{k}}$, which will be characterized below, according to the details of the physical sys-

tem. For definiteness, in our quasi-2D calculations it is assumed that the pairing interaction depends only on the in-plane momenta.

(i) *3D jellium, s -wave symmetry.* We assume a parabolic dispersion relation $\epsilon_{\mathbf{k}} = \mathbf{k}^2/2m - \mu$, with $\varphi_{\mathbf{k}} = (1 + k^2/k_0^2)^{-1/2}$. The parameter k_0 is the inverse range of the interaction and represents a soft cutoff in momentum space for the interaction. As will be clear later, $k_0 > k_F$ is assumed in general in order to access the strong coupling limit. It is convenient to introduce a dimensionless scale g/g_c for the coupling constant. Here, following Ref. 3, we choose $g_c = -4\pi/mk_0$, which corresponds to the critical value of the coupling above which bound pairs are formed in vacuum.

(ii) *2D jellium, s -wave symmetry.* For 2D jellium we choose the same $\epsilon_{\mathbf{k}}$ and $\varphi_{\mathbf{k}}$ as for case (i). We find that $T_c = 0$, in agreement with the Mermin-Wagner theorem. To understand this result, note that the assumption that T_c is finite leads to a contradiction, associated with an unphysical divergence in the pseudogap amplitude. This unphysical result derives from an infrared, logarithmic divergence in the phase space integral on the right-hand side of Eq. (9a). This divergence can be made obvious by rewriting this equation using the low frequency, long wavelength expansion of the T matrix so that

$$\Delta_{\text{pg}}^2 \approx \frac{1}{a_0'} \sum_{\mathbf{q}} b(\Omega_{\mathbf{q}}). \quad (14)$$

Pairing fluctuations, thus, disorder the system for any finite temperature. Even in 2D, for which $T_c = 0$, we obtain a finite pseudogap, as will be seen in Sec. III B. It should be noted that this result is general and remains valid for both s - and d -wave pairing on discrete lattices, as well. This is a consequence of the fact that the lattice energy dispersion is quadratic at sufficiently small wave vectors, so that the same arguments as above can be applied.

(iii) *Quasi-2D jellium, s -wave symmetry.* Here we use $\varphi_{\mathbf{k}}$, as in the previous two cases, and adopt an anisotropic energy dispersion

$$\epsilon_{\mathbf{k}} = \frac{\mathbf{k}_{\parallel}^2}{2m_{\parallel}} + \frac{k_{\perp}^2}{2m_{\perp}} - \mu, \quad (15)$$

where k_{\perp} is restricted to a finite interval ($|k_{\perp}| \leq \pi$),²⁸ while \mathbf{k}_{\parallel} is unconstrained.

By tuning the value of the anisotropy ratio m_{\perp}/m_{\parallel} from one to infinity, this model can be applied to study effects associated with continuously varying dimensionality from 3D to 2D.²⁹ For convenience, we use the parameter g_c derived for 3D jellium, as a scale factor for the coupling strength, and call it g_0 to avoid confusion.

(iv) *Quasi-2D lattice, s - and d -wave symmetry.* In the presence of a lattice we will adopt a simple tight-binding model with dispersion

$$\epsilon_{\mathbf{k}} = 2t_{\parallel}(2 - \cos k_x - \cos k_y) + 2t_{\perp}(1 - \cos k_{\perp}) - \mu, \quad (16)$$

where t_{\parallel} (t_{\perp}) is the hopping integral for the in-plane (out-of-plane) motion. Here we consider both isotropic s -wave pairing symmetry with $\varphi_{\mathbf{k}} = 1$, as in the negative U Hubbard model, as well as d -wave effects with

$$\varphi_{\mathbf{k}} = \cos k_x - \cos k_y. \quad (17)$$

It should be noted that in the lattice case, because the momentum integration is restricted to the first Brillouin zone, it is not necessary to introduce a cutoff for the interaction in momentum space.

III. NUMERICAL RESULTS

Equations (9), together with the various models for $\varphi_{\mathbf{k}}$ and $\epsilon_{\mathbf{k}}$, were solved numerically for Δ_{pg} , μ , and T_c . The numerically obtained solutions satisfy the appropriate equations with an accuracy higher than 10^{-7} . The momentum summations were calculated through numerical integration over the whole \mathbf{k} space for the jellium case, and over the entire Brillouin zone for the lattice. However, to facilitate our calculations in the case of the quasi-2D lattice with a d -wave pairing interaction, the momentum integral along the out-of-plane direction, in general, was replaced by summation on a lattice with $N_{\perp} = 16$ sites. For completeness we compared solutions obtained with and without the low frequency, long wavelength expansions of the T matrix discussed above, and found extremely good agreement between the two different approaches. In general, we chose the ratios $m_{\perp}/m_{\parallel} = 100$ or $t_{\perp}/t_{\parallel} = 0.01$, although higher values of the anisotropy were used for illustrative purposes in some cases.

A. Overview: T_c and effective mass of the pairs

It was pointed out in Ref. 3 in the context of the attractive Hubbard calculations, that the appropriate description of the strong coupling limit corresponds to *interacting* bosons on a lattice with effective hopping integral $t' \approx -2t^2/U$. It, therefore, will necessarily vanish in the strong coupling limit, as $U \rightarrow \infty$. In addition to this hopping, there is an effective boson-boson repulsion which also varies as $V' \approx -2t^2/U$.

This description of a boson Hamiltonian can be related to the present calculations through Eqs. (10)–(12) which represent the Green's function for such a Hamiltonian and its parametrization via the pair mass M^* . By solving Eqs. (9) self-consistently and identifying M^* from the effective pair propagator (or T matrix), our M^* necessarily incorporates all renormalizations such as Pauli principle induced pair-pair repulsion, pairing symmetry and density related effects. Note, in contrast to Ref. 3, in the present work we are not restricted to the bosonic limit, nor is it essential to consider a periodic lattice. Thus, much of this language is also relevant to the moderately strong coupling (but still fermionic) regime, and can even be applied to jellium.

The goal of this subsection is to establish a natural framework for relating M^* to T_c . The parameters which enter into M^* via Eq. (12) vary according to the length scales in the various physical models. In the case of jellium, M^* depends in an important way on the ratio k_0/k_F . For the case of s -wave pairing on a lattice, M^* depends on the inverse lattice constant π/a and density n . Finally, for the case of d -wave pairing, there is an additional length scale introduced as a result of the finite spatial extent of the pair. This enters as if there were an equivalent reduction in k_0/k_F in the analogous jellium model. The following factors act to increase M^* or, alternatively, to reduce the mobility of the pairs: the presence of a periodic lattice, a spatially extended

pairing symmetry (such as d -wave) or, for jellium, small values of the ratio $k_0/k_F \lesssim 0.4$ (i.e., high density).

In order to relate T_c to M^* , we observe that in an ideal Bose-Einstein system T_c is inversely proportional to the mass. Here, this dependence is maintained, in a much more complex theory, as a consequence of Eqs. (9a) and (14). This is essentially an equation for the number of pairs (bosons), with renormalized mass M^* . Thus, as we increase g towards the bosonic regime, it is not surprising that T_c varies inversely with M^* .

This leads to our main observations, which apply to moderate and large g , although not necessarily in the strict bosonic regime. (i) For the general lattice case, we find that T_c vanishes, either asymptotically or abruptly, as the coupling increases, in the same way that the inverse pair mass approaches zero.³⁰ (ii) For the case of jellium or low densities on a lattice, both T_c and M^* remain finite and are inversely proportional. These observations are consistent with, but go beyond, the physical picture in Ref. 3 that T_c is expected to be proportional to the pair hopping integral t' . It should be stressed that in the very weak coupling limit the pair size or correlation length is large. In this case, the motion of the pairs becomes highly collective, so that the effective pair mass is very small.

In the presence of a lattice, the dependence on band filling n is also important for M^* , and thereby, for T_c . We find that the bosonic regime is not accessed for large $n > n_c \approx 0.53$. There are two reasons why superconductivity abruptly disappears within the fermionic regime. This occurs primarily (in the language of Ref. 3) as a consequence of large pair-pair repulsion, relevant for high electronic densities, which leads to large M^* . In addition, there are effects associated with the particle-hole symmetry at half filling.³¹ Precisely at half filling (i.e., the ‘‘filling factor’’ $f = 1/2$, or $2f = n = 1$), for the band structure we consider, there is complete particle-hole symmetry and μ is pinned at E_F . Similarly, in the vicinity of $n = 1$, the chemical potential remains near E_F for very large coupling constants g .

By contrast, in the small density (lattice) limit for the s -wave case ($n \approx 0.1$), pair-pair repulsion is relatively unimportant in M^* and there is no particle-hole symmetry. In this way the bosonic regime is readily accessed. Moreover, in this limit we see a precise scaling of T_c with $1/g$ in the same way as predicted by Ref. 3 (via the parameter $t' = -2t^2/U$). Thus in this low density limit superconductivity disappears asymptotically, rather than abruptly.

The effects of pairing symmetry should also be stressed. Because of the spatial extent of the d -wave function, the pair mobility is strongly suppressed, and, thus, M^* is relatively larger than for the s -wave case. This lower mobility of d -wave pairs leads to the important result that superconductivity is *always abruptly* (rather than asymptotically) destroyed with sufficiently large coupling. Near half filling we find μ remains large when T_c vanishes, at large g . As the density n is reduced, away from half filling, μ decreases somewhat. It is important to note that the system remains in the fermionic regime (with positive μ) for all densities down to $n \approx 0.09$.

In all cases discussed thus far, T_c exhibits a nonmonotonic dependence on the coupling constant. It grows exponentially at small g and shuts off either asymptotically or

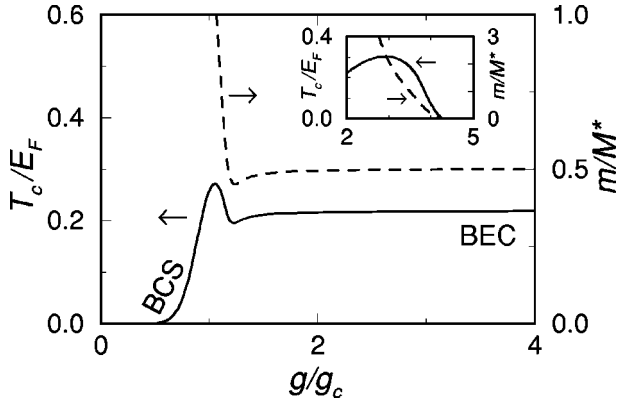


FIG. 1. T_c and m/M^* as a function of g/g_c in the 3D jellium model with $k_0/k_F=4$ (main figure) and $k_0/k_F=1/3$ (inset), corresponding to short range (or low density), and long range interactions (or high density), respectively.

abruptly at higher g . One can view this effect as deriving from a competition between pairing energy scales and effective mass or mobility energy scales. This competition is not entirely dissimilar to that found in more conventional Eliashberg theory where the fermionic renormalized mass and the attractive interaction compete in such a way as to lead to a saturation in T_c at large coupling. However, in the present context, for intermediate and strong coupling, we are far from the Fermi liquid regime and the effective mass of the quasibound or bound pair is a more appropriate variable.

With this background, it should not be surprising that nonmonotonic behavior will arise, even in situations as simple as in jellium models. Indeed, in this case we find that for sufficiently long range interactions or high densities (small k_0/k_F) superconductivity disappears abruptly before the bosonic regime can be reached.³² Even for the case of short range interactions ($k_0/k_F=4$), there is a depression in T_c caused by an increase in the pair mass, while still in the fermionic regime.

In Fig. 1 we plot the calculated T_c for the case of an isotropic, 3D jellium model with s -wave pairing, along with the inverse pair mass m/M^* . This figure is presented primarily as a base line with which to compare subsequent plots. The parameter $k_0/k_F=4$, is reasonably large so that the high g asymptote is found to reach the ideal Bose-Einstein limit ($T_c=0.218E_F$) with $M^*=2m$. The approach to the high g asymptote is from below, as is expected.⁷ This is a result of the decreasing Pauli principle repulsion associated with increasing g , and concomitant reduction in pair size. The non-monotonic behavior at intermediate $g/g_c \approx 1$ can be associated with structure in the effective pair mass, and has been discussed previously from a different perspective.¹³

In the inset are plotted analogous curves for the case of long range interactions or high densities ($k_0/k_F=1/3$). This figure illustrates how superconductivity vanishes abruptly before the bosonic regime is reached, as a consequence of a diverging pair mass.³²

B. Effects of dimensionality

In this subsection we illustrate the effects of anisotropy or dimensionality on T_c (and on Δ_{pg} and μ) within the context of a jellium dispersion.³³ A particularly important check on

our theoretical interpolation scheme is to ascertain that T_c is zero in the strict 2D limit and that μ varies continuously from E_F in weak coupling to the large negative values characteristic of the strong coupling bosonic limit. The present calculational scheme should be compared with that of Yamada and co-workers¹⁷ who included “mode coupling” or feedback contributions to T_c , but only at the level of the lowest order “box” diagram discussed in Ref. 12. These authors were unable to find a smooth interpolation between weak and strong coupling, but did successfully repair the problems^{14,15} associated with the NSR scheme, which led to negative μ even in arbitrarily weak coupling.

Figures 2(a) and 2(b) show the effect on T_c and on Δ_{pg} and μ , respectively, of introducing a layering or anisotropy into jellium with s -wave pairing. The various curves correspond to different values of the anisotropy ratio m_{\perp}/m_{\parallel} . It can be seen from these two figures that T_c approaches zero as the dimensionality approaches 2. At the same time the chemical potential μ interpolates smoothly from the Fermi energy at weak coupling towards zero at around $g/g_0=1.5$ to large negative values (not shown) at even larger g . The vanishing of the superconducting transition in strictly 2D was discussed in detail in Sec. II.

It should be noted that quasi-two dimensionality will be an important feature as we begin to incorporate the complexity of d -wave pairing. The essential physics introduced by decreasing the dimensionality is the reduction in energy scales for T_c . The chemical potential and pseudogap amplitude are relatively unaffected by dimensional crossover effects.³⁴ While T_c rapidly falls off when anisotropy is first introduced into a 3D system (such as is plotted in Fig. 1), the approach to the strict 2D limit is logarithmic and therefore slow, as can be seen explicitly in Fig. 2(c). Thus, in this regime, to get further significant reductions in T_c associated with a dimensionality reduction requires extremely large changes in the mass anisotropy.

C. Effects of a periodic lattice

The first applications of a BCS Bose-Einstein crossover theory to a periodic lattice were presented in Ref. 3. The present approach represents an extension of the NSR theory in two important ways: we introduce mode coupling or full self-energy effects which are parametrized by Δ_{pg} , and which enter via Eq. (9a). Moreover, the number equation [see Eq. (9c), which is a rewriting of Eq. (4d) in terms of Δ_{pg}] is evaluated by including self-energy effects to all orders. This is in contrast to the approximate number equation used in Ref. 3, which includes only the first order correction. In this way we are able to capture the effects which were qualitatively treated by these authors and which are associated with the lattice.

Figure 3(a) plots the behavior of T_c (solid line) in an isotropic three-dimensional lattice (with s -wave pairing, $\varphi_{\mathbf{k}}=1$) at a low density $n=0.1$. The effects of higher electronic filling are shown in the inset. The low n behavior in the main portion of the figure can be compared with the jellium calculations of Fig. 1. For small n , T_c decreases asymptotically to zero at high g . For larger n , T_c vanishes abruptly before the bosonic regime ($\mu<0$) is reached [see inset of Fig. 3(b)]. These various effects reflect the analogous reduction in

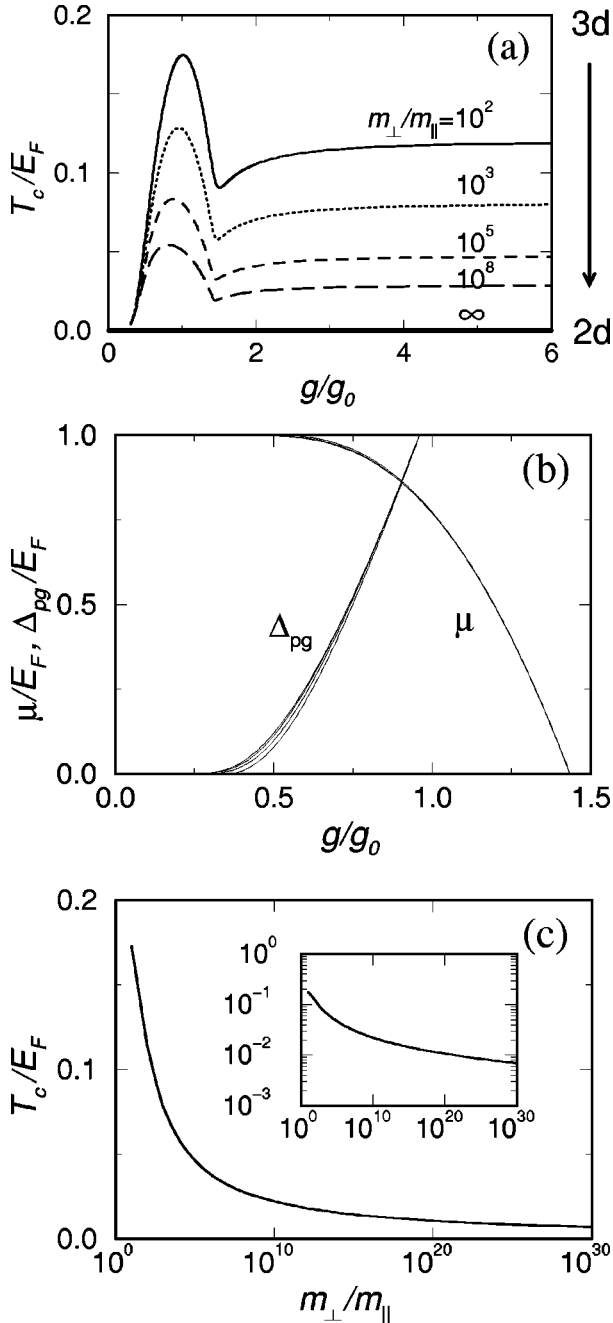


FIG. 2. Dimensionality crossover in a quasi-2D jellium model. (a) T_c as a function of g is seen to vanish for all g as $m_\perp/m_\parallel \rightarrow \infty$, while (b) μ and Δ_{pg} change little. A continuous variation of T_c versus m_\perp/m_\parallel at $g/g_0=4$ is shown in the main portion (semi-log plot) and the inset (log-log plot) of (c). Here $k_0/k_F=4$, $g_0 \equiv -4\pi/mk_0$.

the effective pair mobility, parametrized by the inverse pair mass m/M^* . To see the correlation with m/M^* in the low density limit, we plot this quantity in Fig. 3(b), for the lattice as well as jellium case (where for the latter, $m/M^* \rightarrow 1/2$ at large g). Here the coupling constants are indicated in terms of g/g_c for jellium and $-g/6t$ for the lattice. The inflection points at $-g/6t \approx 2$ in both T_c and m/M^* curves correspond to $\mu=0$, which marks the onset of the bosonic regime.

Also plotted in both Figs. 3(a) and 3(b) (dashed lines) is the effective hopping $t' = -2t^2/g$ for $n=0.1$, rescaled such

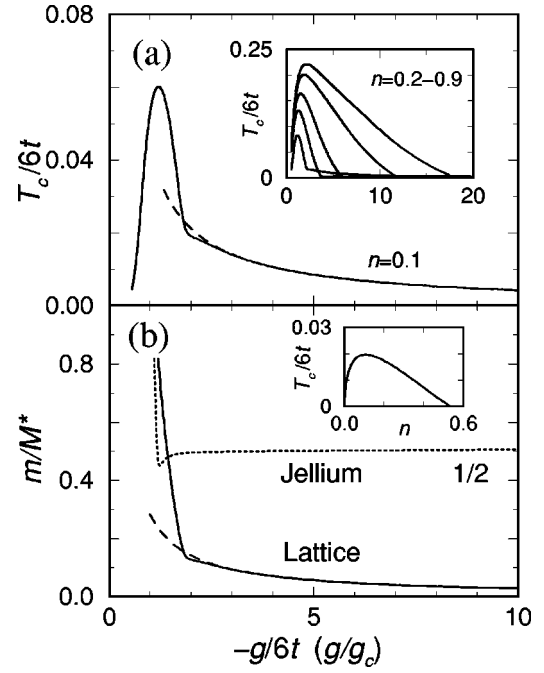


FIG. 3. (a) T_c and (b) m/M^* (solid lines) vs g at low filling ($n=0.1$) on a 3D lattice, and T_c at larger filling in the inset of (a). A fit to the functional form $t' = -2t^2/g$ is plotted (dashed lines) in (a) and (b) with adjusted proportionality constants. For comparison, m/M^* vs g/g_c for 3D jellium (Fig. 1) is replotted (dotted line) in (b). From bottom to top, the inset of (a) shows T_c for densities $n=0.2, 0.5, 0.7, 0.85$, and 0.9 . The inset of (b) shows T_c at $\mu=0$ as a function of n .

that it coincides with T_c and m/M^* , respectively, at high coupling ($-g/6t=30$). This figure illustrates clearly the effect first noted by Nozières and Schmitt-Rink that in the entire bosonic regime, T_c varies with high precision as t' or equivalently as m/M^* .

Finally, in the inset of Fig. 3(b), we demonstrate the limiting value of n , above which the bosonic limit cannot be accessed. What is plotted here is the value of T_c at which μ is zero as a function of density n . This figure indicates that the bosonic regime cannot be reached for $n > n_c \approx 0.53$. At densities higher than this, the pair-pair repulsion increases M^* sufficiently, so that T_c vanishes abruptly, while μ is still positive.

D. Effects of d -wave symmetry

We now introduce the effects of a d -wave pairing interaction. For the purposes of comparison we begin by illustrating T_c for the case of s -wave pairing on an anisotropic lattice, shown in Fig. 4(a), for three different values (0.7, 0.85, and 0.9) of the density n .³⁵ The inset indicates the behavior of the pseudogap magnitude and the chemical potential. The plots of Δ_{pg} for the three different n are essentially unresolvable in the figure. Note, from the inset, that within small numerical errors T_c and μ vanish simultaneously. A comparison of the magnitude of T_c (in the main figure) with the 3D counterpart shown in the inset of Fig. 3(a) illustrates how T_c is suppressed by quasi-two dimensionality.³⁶

In Fig. 4(b), similar plots are presented for the d -wave case. Here we use the same values of the filling factor as in

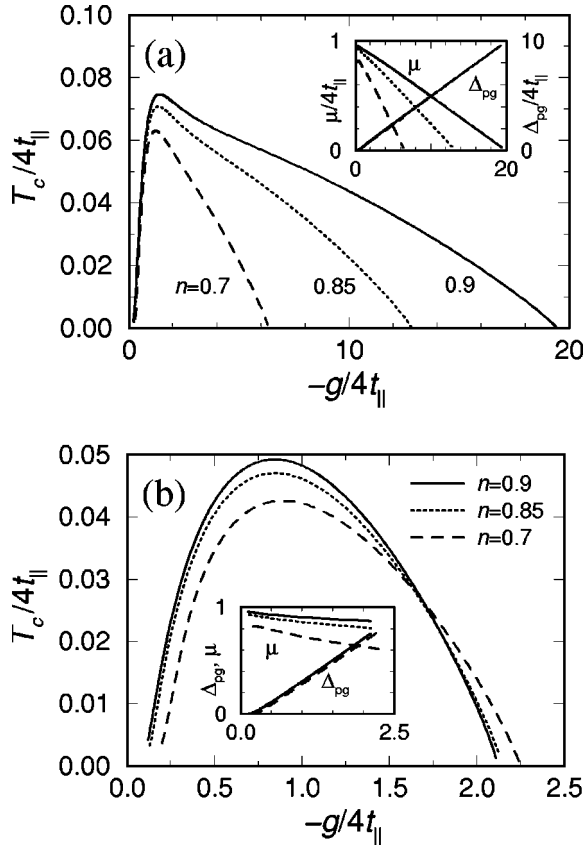


FIG. 4. Lattice effects on T_c (main figure) and μ and Δ_{pg} (inset) as a function of g for $n=0.7$ (dashed lines), 0.85 (dotted lines), and 0.9 (solid lines) in quasi-2D for (a) s -wave and (b) d -wave pairing symmetries. Here $t_{\perp}/t_{\parallel}=0.01$. In (b), T_c vanishes at a much smaller g than does its s -wave counterpart.

Fig. 4(a), to which Fig. 4(b) should be compared. The essential difference between the two figures is the large g behavior. Lattice effects produce the expected cutoff for s -wave pairing. In the d -wave situation this cutoff is at even smaller g , and moreover, corresponds to $\mu \approx E_F$. Calculations similar to those shown in the inset of Fig. 3(b) indicate that superconductivity disappears while μ remains positive for all n above the extreme low density limit (i.e., for $n > n_c \approx 0.09$).²³ This behavior is in contrast to that of the s -wave case where $n_c \approx 0.53$.

In the d -wave case, the pair size cannot be made arbitrarily small, no matter how strong the interaction. As a result of the extended size of the pairs, residual repulsive interactions play a more important role. In this way, the pair mobility is reduced and the pair mass increased. Thus, as a consequence of the finite pair size, *in the d -wave case the system essentially never reaches the superconducting bosonic regime.*

E. Phase diagrams

In this section we introduce an additional energy scale T^* , and in this way, arrive at plots of characteristic “phase diagrams” for the crossover problem. Our focus is on the pseudogap onset, so that attention is restricted to relatively small and intermediate coupling constants g ; consequently, the bosonic regime is not addressed. Here, our calculations

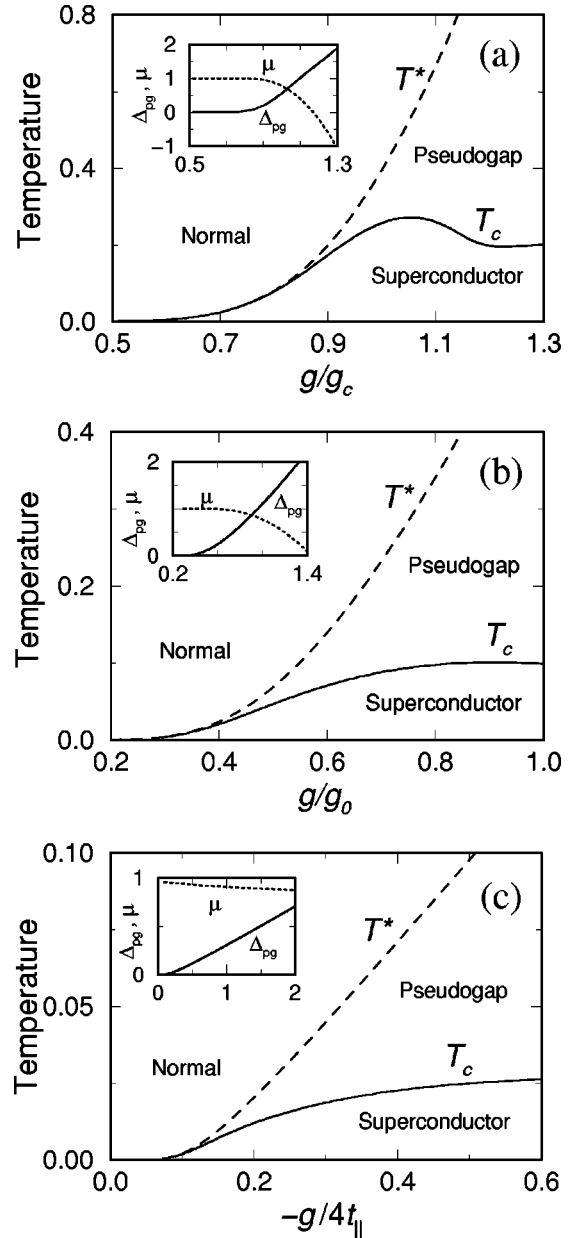


FIG. 5. Phase diagrams of (a) 3D jellium ($k_0/k_F=4$), quasi-2D jellium ($k_0/k_F=4$, $m_{\perp}/m_{\parallel}=10^4$), (c) a d -wave symmetry on a quasi-2D lattice ($t_{\perp}/t_{\parallel}=10^{-4}$). Here we take $n=0.9$. The same energy units are (a), (b) E_F and (c) $4t_{\parallel}$.

of T^* are based on the solution of Eq. (9b), along with Eq. (9c), under the assumption that $\Delta_{pg}=0$. This approximation for T^* is consistent with more detailed numerical work¹³ in which this temperature is associated with the onset of a pair resonance in the T matrix.

In Figs. 5(a)–5(c) our results are consolidated into phase diagrams for the different physical situations. The case of 3D jellium, with s -wave pairing [Fig. 5(a)] is presented primarily as a point of comparison. Figure 5(b) corresponds to quasi-2D jellium ($m_{\perp}/m_{\parallel}=10^4$), with s -wave pairing and Fig. 5(c) to the case of d -wave pairing in a quasi-2D lattice case ($t_{\perp}/t_{\parallel}=10^{-4}$).³⁷ The insets indicate the behavior of μ and Δ_{pg} . Comparing T^* with T_c represents a convenient way of determining the onset of the pseudogap state. (For definiteness, we define the onset to correspond to T^*

$=1.1T_c$.) It is clear from the first two figures that this occurs for 3D jellium at $g/g_c \approx 0.9$, and for the quasi-2D case at $g/g_0 \approx 0.4$.³⁸ This observation reinforces the notion that pseudogap effects are easier to come by in lower-dimensional systems. Similar behavior is seen in the quasi-2D lattice situation for the d -wave case, although the energy scales on the horizontal and vertical axes reflect the parameter t_{\parallel} (rather than g_c and E_F).

IV. IMPLICATIONS FOR THE CUPRATES

There has been much concern in the literature about whether generalized BCS Bose-Einstein crossover theories are relevant to the copper oxide superconductors. Is the coupling g sufficiently “large” in some sense to warrant this form of departure from conventional BCS theory? In more concrete terms, one may ask if the calculated energy scales for Δ_{pg} , μ , T^* , and T_c are consistent with experiment? Are there other effects which are more important than is the role of small ξ ? Perhaps among the most intriguing questions raised is how does one incorporate hole concentration (denoted by x) dependences into this picture?

An early motivation for adopting these crossover approaches was the observed short coherence length ξ , which was suggestive of some form of “real space pairing.” It is also clear that these systems are doped Mott insulators³⁹ so that the metal insulator transition at 1/2 filling ($x=0$) should be integrated into any theoretical approach. This transition is generally^{40,41} parametrized through an “order parameter” such as the plasma frequency ω_p which must necessarily vanish as $x \rightarrow 0$. Finally, it should be noted that there are no dramatic effects on ξ with variable x .⁴²

It is clear that, in any attempt to understand pseudogap phenomena in the cuprates, both the small size of ξ and that of ω_p should be addressed on an equal footing. Early work by our group⁴³ investigated the effects of small ω_p on the crossover problem, at the level of the Nozières–Schmitt-Rink approximation, for charged fermions. Coulomb interactions were treated in the RPA in parallel with the RPA-like ladder diagrams of the particle-particle attraction. These early calculations established that deviations from the BCS limit were more pronounced, the smaller the plasma frequency. Thus, for the same value of g , proximity to the insulating state is correlated with a tendency towards “bosonic” superconducting transitions. Additional effects (in the same direction) result from the likely decrease in dimensionality as the insulator is approached. Both of these effects, thus, suggest an amplification of pseudogap phenomena as $x \rightarrow 0$.

In this section we address two issues which have been raised as relevant for the cuprates: we examine the size of the various energy scales for the case of d -wave superconductors (all of which depend on the hopping matrix element t_{\parallel}), and we discuss some aspects of the hole concentration dependence of the phase diagram, beyond the very general qualitative issues which have been noted above. It should be stressed that the fundamental basis of all crossover theories is mechanism independent. No information is used or assumed about the details of the pairing mechanism beyond the existence of a pairing coupling constant g . In almost any microscopically based pairing scenario, g is likely to contain

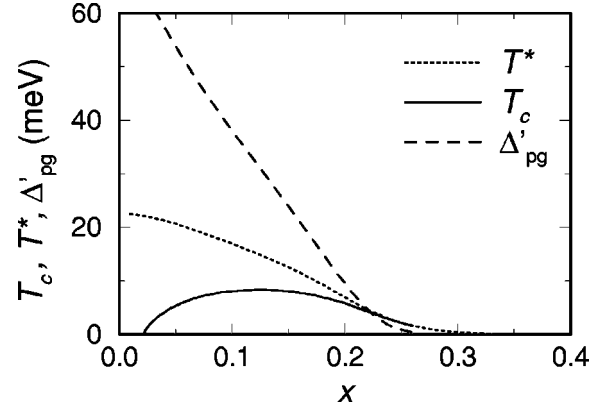


FIG. 6. Doping dependence of T_c , T^* , and Δ'_{pg} [$\equiv 2\Delta_{pg}$, the magnitude of the pseudogap at $(\pi, 0)$]. Here $t_{\perp}/t_{\parallel}=0.01$, $t_0=0.5$ eV, and g is assumed constant, while the symmetry is d -wave.

some degree of x dependence. However, since there is no consensus on the pairing mechanism, in the present paper it is inappropriate to obscure our general results by making any detailed assumptions about the nature of $g(x)$.

Here we focus exclusively on the x dependence of the underlying metal-insulator transition. We take g as doping independent (which is not unreasonable in the absence of any more detailed information) and incorporate the Mott transition at half-filling, by introducing an x dependence into the in-plane hopping matrix elements t_{\parallel} of our calculations. In this way, we can explore the question of the size of the various energy scales and capture some degree of hole concentration dependence, albeit not the entire effect. Our renormalized band structure is based on the limit of extremely strong on-site Coulomb repulsion, as seems appropriate for representing the Mott transition. It follows from very early work on the Hubbard model³⁹ that the hopping matrix element is renormalized as $t_{\parallel}(x) \approx t_0(1-n) = t_0x$, where $t_0(\approx 0.5$ eV) is the matrix element in the absence of Coulomb effects. Equivalently, the effective particle mass varies as $1/x$. This change of energy scale is consistent with the requirement that the plasma frequency vanish at $x=0$.⁴⁴

In Fig. 6 we replot the d -wave phase diagram of Fig. 4(b) for the case of fixed $-g/4t_0=0.045$ (and $t_{\perp}/t_{\parallel}=0.01$), which is chosen to fit the measured size of the pseudogap at T_c for extremely underdoped cuprates.⁴⁵ Shown in the figure are T^* , Δ_{pg} , and T_c . Agreement with experiment may or may not be fortuitous since the coupling constant was assumed to be independent of x . Nevertheless, the energy scales appear to be consistent with those measured experimentally^{46–50} and the x dependent trends are not inconsistent.⁵¹

It should be stressed that the results shown in the figure are robust consequences of our crossover theory. As a result of d -wave symmetry, T_c vanishes at moderately strong coupling. Moreover, this maximal coupling is a fairly universal number (i.e., independent of n) for a given t_{\parallel} , over the physical range of hole concentrations ($x < 0.3$) [see, e.g., Fig. 4(b)]. Once a linear x dependence is enforced in t_{\parallel} , near half filling, T_c decreases naturally as x decreases, and vanishes for extremely low doping concentration. This feature is insensitive to the detailed parametrizations of the model.

V. CONCLUSIONS

In this paper we have applied a previously discussed^{12,13} BCS Bose-Einstein crossover theory to complex situations which are more physically relevant than are our earlier studies of 3D *s*-wave jellium. In this way, we have determined the effects of quasi-two dimensionality, of periodic discrete lattices, and of a *d*-wave pairing interaction. This crossover theory yields results which appear consistent with known physical constraints and plausibility arguments. Thus, in particular, our strict 2D calculations yield a sensible interpolation scheme (for μ) with T_c strictly zero. The effects of the lattice are consistent with earlier Monte Carlo and other approaches, yielding a vanishing strong coupling limit for T_c associated with an increase (with g) of the effective mass M^* of the fermion pairs. Finally our *d*-wave studies reveal that, for this symmetry, the superconducting bosonic regime is essentially never reached. T_c is suppressed to zero at moderate coupling constants, presumably because of the lowered pair mobility due to the constraints imposed by *d*-wave symmetry: the pair size cannot be reduced beyond the scale of a lattice spacing. These features should be appended to other observations in the literature² which note that in the strong coupling limit a *d*-wave superconductor will not exhibit gap nodes. Indeed, it is sometimes argued that this provides a

“proof” that the cuprates (which exhibit explicit *d*-wave symmetry) cannot be in the bosonic regime. Our results appear to make this case even more strongly, since we find that T_c will be zero whenever a *d*-wave system is in the preformed pair limit.

Our paper includes a brief discussion of the relevance to the copper oxide superconductors, wherein we impose the simplest possible ingredients of a Mott transition to arrive at some indications of hole concentration dependence and characteristic energy scale parameters, such as T_c , T^* , and the pseudogap amplitude Δ_{pg} . The numbers which emerge seem to be reasonably consistent with experiment, although we have made no assumptions about the origin or hole concentration dependence of the pairing interaction. In this way, one may argue that these crossover scenarios provide useful insights into the pseudogap state of the cuprates.

ACKNOWLEDGMENTS

We would like to thank M. Norman and B. Gyorffy for useful discussions. This research was supported in part by the Science and Technology Center for Superconductivity funded by the National Science Foundation under Award No. DMR 91-20000.

-
- ¹D. M. Eagles, Phys. Rev. **186**, 456 (1969).
²A. J. Leggett, J. Phys. (Paris) **41**, C7/19 (1980).
³P. Nozières and S. Schmitt-Rink, J. Low Temp. Phys. **59**, 195 (1985).
⁴Y. J. Uemura, L. P. Le, G. M. Luke, B. J. Sternlieb, W. D. Wu, J. H. Brewer, T. M. Riseman, C. L. Seaman, M. B. Maple, M. Ishikawa, D. G. Hinks, J. D. Jorgensen, G. Saito, and H. Yamochi, Phys. Rev. Lett. **66**, 2665 (1991).
⁵M. Randeria, J.-M. Duan, and L.-Y. Shieh, Phys. Rev. Lett. **62**, 981 (1989).
⁶R. Micnas, M. H. Pedersen, S. Schafroth, T. Schneider, J. J. Rodriguez-Nunez, and H. Beck, Phys. Rev. B **52**, 16 223 (1995).
⁷R. Haussmann, Z. Phys. B **91**, 291 (1993); Phys. Rev. B **49**, 12 975 (1994).
⁸J. Ranninger and J. M. Robin, Phys. Rev. B **53**, R11 961 (1996).
⁹E. V. Gorbar, V. M. Loktev, and S. G. Sharapov, Physica C **257**, 355 (1996); V. P. Gusynin, V. M. Loktev, and S. G. Sharapov, JETP Lett. **65**, 182 (1997); F. Pistolesi and G. C. Strinati, Phys. Rev. B **49**, 6356 (1994).
¹⁰L. P. Kadanoff and P. C. Martin, Phys. Rev. **124**, 670 (1961).
¹¹B. R. Patton, Ph.D. thesis, Cornell University, 1971; Phys. Rev. Lett. **27**, 1273 (1971).
¹²B. Janko, J. Maly, and K. Levin, Phys. Rev. B **56**, R11 407 (1997).
¹³J. Maly, B. Janko, and K. Levin, cond-mat/9805018 (unpublished). See also I. Kosztin, Q. Chen, B. Jankó, and K. Levin, Phys. Rev. B **58**, R5936 (1998); Q. Chen, I. Kosztin, B. Jankó, and K. Levin, Phys. Rev. Lett. **81**, 4708 (1998).
¹⁴S. Schmitt-Rink, C. M. Varma, and A. E. Ruckenstein, Phys. Rev. Lett. **63**, 445 (1989).
¹⁵J. W. Serene, Phys. Rev. B **40**, 10 873 (1989).
¹⁶Sofo and Balseiro tried to repair this in 2D. See J. O. Sofo and C. A. Balseiro, Phys. Rev. B **45**, 8197 (1992).
¹⁷A. Tokumitsu, K. Miyake, and K. Yamada, Physica B **165-166**, 1039 (1990); J. Phys. Soc. Jpn. **60**, 380 (1991); Phys. Rev. B **47**, 11 988 (1993).
¹⁸L. Belkhir and M. Randeria, Phys. Rev. B **45**, 5087 (1992).
¹⁹N. Trivedi and M. Randeria, Phys. Rev. Lett. **75**, 312 (1995); J. M. Singer, M. H. Pedersen, and T. Schneider, Physica B **230**, 955 (1997); J. M. Singer, M. H. Pedersen, T. Schneider, H. Beck, and H. G. Matuttis, Phys. Rev. B **54**, 1286 (1996).
²⁰B. L. Gyorffy, J. B. Staunton, and G. M. Stocks, Phys. Rev. B **44**, 5190 (1991).
²¹M. Randeria, J.-M. Duan, and L.-Y. Shieh, Phys. Rev. B **41**, 327 (1990).
²²J. R. Engelbrecht, A. Nazarenko, M. Randeria, and E. Dagotto, Phys. Rev. B **57**, 13 406 (1998).
²³In the limit of unphysically small $n < 0.09$ the superconducting bosonic regime can be accessed for certain couplings, since the lattice and jellium models then become indistinguishable, and the internal structure of the pairs (dominated by the pairing symmetry) becomes less important.
²⁴In spite of the asymmetric form in which the dressed and bare Green's functions enter the equations in the present theory, it can be shown, following arguments along the lines of G. Baym and L. P. Kadanoff, Phys. Rev. **124**, 287 (1961), that the conservation law for particle number is obeyed. The derivation of the conservation laws for energy, momentum and angular momentum [V. Ambegaokar and B. Patton (private communication)] depends on the use of the equations of motion, rather than criterion *B* in the above reference. Moreover, the thesis by Patton establishes quite clearly how to apply the generalized Ward identity to construct a conserving approximation for the two particle (electromagnetic) response functions.

- ²⁵M. R. Norman, H. Ding, M. Randeria, J. C. Campuzano, T. Yokoya, T. Takeuchi, T. Takahashi, T. Mochiku, K. Kadowaki, P. Guptasarma, and D. G. Hinks, *Nature (London)* **392**, 157 (1998).
- ²⁶J. Maly, B. Janko, and K. Levin, *Phys. Rev. B* **59**, 1354 (1999).
- ²⁷J. Maly, Ph.D. thesis, The University of Chicago, 1997.
- ²⁸We emphasize that a cutoff for k_{\perp} is crucial for the quasi-two dimensionality of the system; otherwise, by rescaling $k_{\perp} \rightarrow (m_{\perp}/m_{\parallel})^{1/2} k_{\perp}$, the system can be transformed into an isotropic 3D jellium model.
- ²⁹Strictly speaking, a very large cutoff Λ for k_{\perp} or a very low particle density (i.e., $k_F \ll \Lambda$) is necessary to restore the 3D limit if $m_{\perp}/m_{\parallel}=1$ is fixed. Alternatively, 3D can be achieved by letting $m_{\perp}/m_{\parallel} \rightarrow 0$ while fixing Λ . This complication does not occur for the lattice case, where all momenta are restricted within the first Brillouin zone.
- ³⁰This is a high density effect at strong coupling. Lattice band structure effects and d -wave pairing serve to enhance this behavior. Moreover, it should be noted that the pseudogap $\Delta_{pg} \propto [T_c/(m/M^*)]^{3/2}$ remains finite as both T_c and m/M^* approach zero.
- ³¹In a negative U Hubbard model, there also exists a competition between superconductivity and charge-density wave ordering. This may not be relevant for a d -wave pairing interaction.
- ³²In some cases we find T_c may be reentrant, at larger g .
- ³³One may argue that this quasi-2D system is not physical because the kinetic energy in the perpendicular direction should have a band structure, i.e., $2t_{\perp}(1 - \cos k_{\perp})$ instead of being simply $k_{\perp}^2/2m_{\perp}$. In fact, it can be shown analytically that in this case, $M_{\perp}^*/M_{\parallel}^* \propto (m_{\perp}/m_{\parallel})^2$ (instead of m_{\perp}/m_{\parallel}), i.e., the pairs see a magnified anisotropy. This does not affect the conclusion here.
- ³⁴The onset coupling g for the pseudogap decreases when the dimensionality is reduced, and eventually vanishes in strictly 2D.
- ³⁵We show results for these values of n because they correspond to overdoped, optimally doped, and underdoped cuprates, respectively.
- ³⁶As in the 3D (s -wave) lattice case, the bosonic regime can be accessed at $n < n_c \approx 0.53$ for sufficiently strong coupling.
- ³⁷The phase diagram for the quasi-2D s -wave lattice case is similar to that of the quasi-2D d -wave case.
- ³⁸Note here $g_0 = g_c$.
- ³⁹G. Baskaran, Z. Zou, and P. W. Anderson, *Solid State Commun.* **63**, 973 (1987).
- ⁴⁰P. A. Lee and X. G. Wen, *Phys. Rev. Lett.* **78**, 4111 (1997).
- ⁴¹V. Emery and S. A. Kivelson, *Nature (London)* **374**, 434 (1995).
- ⁴²M. A. Hubbard, M. B. Salamon, and B. W. Veal, *Physica C* **259**, 309 (1996).
- ⁴³J. Maly, K. Levin, and D. Z. Liu, *Phys. Rev. B* **54**, 15 657 (1996).
- ⁴⁴ ω_p may vanish with a different power of x . See J. Orenstein, G. A. Thomas, A. J. Millis, S. L. Cooper, D. H. Rapkine, T. Timusk, L. F. Schneemeyer, and J. V. Waszczak, *Phys. Rev. B* **42**, 6342 (1990).
- ⁴⁵We take $\Delta_{pg} \approx 30$ meV [note $|\varphi_{\mathbf{k}}|=2$ at $(\pi, 0)$ in our convention] at T_c for $x \approx 0.05$ and $t_0 \approx 0.5$ eV for definiteness.
- ⁴⁶H. Ding, T. Yokoya, J. C. Campuzano, T. Takahashi, M. Randeria, M. R. Norman, T. Mochiku, K. Kadowaki, and J. Giapintzakis, *Nature (London)* **382**, 51 (1996).
- ⁴⁷A. G. Loeser, Z.-X. Shen, D. S. Dessau, D. S. Marshall, C. H. Park, P. Fournier, and A. Kapitulnik, *Science* **273**, 325 (1996).
- ⁴⁸H. Ding, J. C. Campuzano, M. R. Norman, M. Randeria, T. Yokoya, T. Takahashi, T. Takeuchi, T. Mochiku, K. Kadowaki, P. Guptasarma, and D. G. Hinks, *J. Phys. Chem. Solids* **59**, 1888 (1998).
- ⁴⁹N. Miyakawa, P. Guptasarma, J. F. Zasadzinski, D. G. Hinks, and K. E. Gray, *Phys. Rev. Lett.* **80**, 157 (1998).
- ⁵⁰M. Oda, K. Hoya, R. Kubota, C. Manabe, N. Momono, T. Nakanano, and M. Ido, *Physica C* **281**, 135 (1997).
- ⁵¹There are some experimental variations from paper to paper. See Refs. 46–50.